A model for large amplitude oscillations of coated bubbles accounting for buckling and rupture

Philippe Marmottant,[a] Sander van der Meer, Marcia Emmer, and Michel Versluis
Department of Science and Technology, University of Twente, P.O. Box 217, 7500AE Enschede, The Netherlands

Nico de Jong
Department of Science and Technology, University of Twente, P.O. Box 217, 7500AE Enschede, The Netherlands and Department of Experimental Echocardiography, Thoraxcentre, Erasmus MC, Rotterdam, The Netherlands

Sascha Hilgenfeldt[b] and Detlef Lohse
Department of Science and Technology, University of Twente, P.O. Box 217, 7500AE Enschede, The Netherlands

(Received 31 March 2005; revised 25 August 2005; accepted 13 September 2005)

We present a model applicable to ultrasound contrast agent bubbles that takes into account the physical properties of a lipid monolayer coating on a gas microbubble. Three parameters describe the properties of the shell: a buckling radius, the compressibility of the shell, and a break-up shell tension. The model presents an original non-linear behavior at large amplitude oscillations, termed compression-only, induced by the buckling of the lipid monolayer. This prediction is validated by experimental recordings with the high-speed camera Brandaris 128, operated at several millions of frames per second. The effect of aging, or the resultant of repeated acoustic pressure pulses on bubbles, is predicted by the model. It corrects a flaw in the shell elasticity term previously used in the dynamical equation for coated bubbles. The break-up is modeled by a critical shell tension above which gas is directly exposed to water. © *2005 Acoustical Society of America.*
[DOI: 10.1121/1.2109427]

PACS number(s): 43.25.Yw, 43.35.Ei [AJS] Pages: 3499–3505

I. INTRODUCTION

To enhance ultrasound echographic imaging, micrometric coated bubbles are used as contrast agents. Coating materials include lipid monolayers, polymer shells, or thick solid shells. The coating stabilizes the bubbles and prevents their coalescence. Pulmonary alveoli in the lungs have a lipidic coating for the same reason.[1] The coating modifies the effective surface tension. Since surface tension plays a crucial role in the dynamics of small bubbles, when the capillary pressure term is of the order of the static ambient pressure, the coating is expected to strongly influence the dynamics.

All current models developed to describe coated bubble oscillations implicitly assume small deformations of the bubble surface: however, in practice, insonifying contrast agent bubbles produces oscillations with large variations in the surface area. We will present in this article a model designed to incorporate the effect of a coating on the microbubble response to ultrasound, and to specifically capture the high-amplitude dynamics.

We focus on phospholipidic monolayer coatings, used in several contrast agent bubbles.[2] The phospholipid molecules naturally adsorb to the interface[3] and shield the water from the air, reducing the surface tension σ to a value lower than that of pure water (73 mN/m). Surface tension can be measured in a flat monolayer with the Langmuir-Blodgett balance, or on centimetric bubbles,[4] showing its dependence on the surface concentration of molecules.

The compression of the monolayer decreases the area available per molecule. When this area reaches that covered by the lipid molecules (typically 0.4 nm^2 for phospholipids in the transconfiguration normal to the interface), the effective surface tension decreases sharply, see Fig. 1. The variation of surface tension with the area A is expressed with the elastic compression modulus defined by $\chi = A(d\sigma/dA)$ (of order 0.2 N/m for a slow compression, as derived from the steepest slopes of Fig. 1). Further compression leads to an unstable situation where the monolayer buckles out of plane, while the surface tension nearly vanishes. A spectacular demonstration of the buckling is the appearance of wrinkles on coated bubbles when their gas dissolves out.[8] Buckling can be reversible.[9,10] Vanishing surface tensions were revealed by the microscopic observation of bubbles with a monolayer lipid coating in a solid state: these bubbles could assume a steady nonspherical shape[11] when deformed with a micropipette, and dissolution was greatly reduced by the absence of the capillary overpressure.[12]

In contrast, a slow expansion separates molecules from each other: surface tension rises. A monolayer made from pure lipid (one species only) will show phase changes from a

[a]Present address: Laboratoire de Spectrométrie Physique, CNRS-Université Joseph Fourier, Boîte Postale 87, F-38402 Saint Martin d'Hères, France.
[b]Present address: Engineering Sciences and Applied Mathematics and Department of Mechanical Engineering, Northwestern University, 2145 Sheridan Road, Evanston, IL 60208.

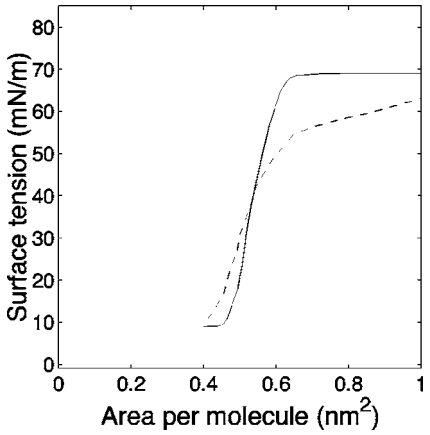

FIG. 1. Effective surface tension versus area per molecule at the interface for two phopholipids (both present in the contrast agent SonoVue®) (see Ref. 5) under *slow compression* at a few percent per minute: distearoylphosphatidylcholine, solid line; and dipalmytoylphosphatidylglycerol, broken line. Curves redrawn from Ref. 6 and 7.

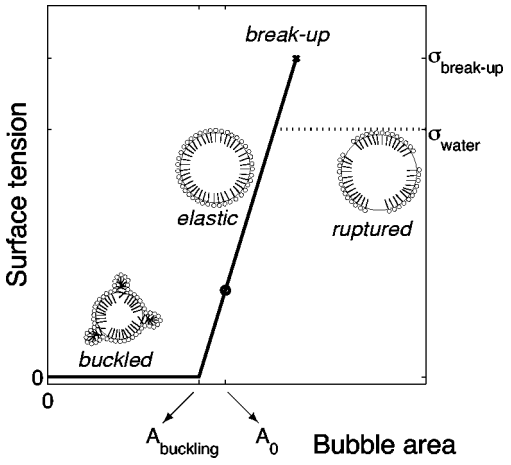

FIG. 2. Model for the dynamic surface tension of a monolayer coated bubble (continuous line). The coating has a fixed number of lipid molecules, which corresponds to a monolayer at equilibrium (when area is A_0). The tension saturates to the water value σ_{water} (broken line) after the break-up tension has been reached ($\sigma_{break-up} > \sigma_{water}$).

two-dimensional (2D) solid state, to a liquid and eventually gaseous state, where surface tension is close to that of water. With a mixture of lipid molecules the phase changes are not necessarily present, and a 2D solid can rupture during expansion, leaving rafts of solid phospholipid molecules separated by clean interfaces.[13]

Most previous existing experimental data on phospholipidic monolayers were collected at very slow compression/expansion rates, when molecules at the interface could equilibrate. Only a few experiments tackled the high-frequency and thus out-of-equilibrium trends: the buckling surface tension comes closer to zero and the elastic modulus becomes higher (see reported experiments[1] with pulmonary surfactant compressed within 0.2 s). These findings give some hint to the extrapolation of surface properties to the realm of high frequency oscillations, the one we are going to explore with oscillating contrast agent bubbles.

II. MODEL

A. Effective surface tension of a bubble during its oscillation

At high frequencies, we propose to model the effective surface tension σ of the lipidic monolayer of a bubble along three linear regimes inspired from the low frequency observations. The regimes depend on the bubble area $A=4\pi R^2$, with R the bubble radius (see Fig. 2). This simplified model is designed to capture the coated bubble dynamics with a minimum of parameters.

The model has three parameters only to describe the surface tension: the buckling area of the bubble $A_{buckling}$ below which the surface buckles, an elastic modulus χ that gives the slope of the elastic regime. The third parameter is incorporated to describe the moment of rupture: the elastic regime holds until a critical break-up tension called $\sigma_{break-up}$. When this limit has been reached the maximum surface tension saturates at σ_{water}.

We motivate here the modeling of the three states.

- Buckled state, $\sigma=0$.

  Consistent with experimental findings on the fast compression of pulmonary phospholipid monolayers, we assume a near vanishing surface tension in the buckled state.[1] The buckling area of the bubble depends on the number n of lipid molecules at the interface and on the molecular area at buckling $a_{buckling}$, with $A_{buckling}=na_{buckling}$, with $a_{buckling}$ typically of the order of 0.4 nm^2, see previous section. Note that a first compression of the bubble might *expel* in bulk some molecules into the bulk,[14] decreasing the number n. After this transient expulsion, and for moderate driving amplitudes and short exposures, we expect the number of molecules to remain constant, as phospholipids with long carbon chains are poorly soluble.
- Elastic state, $\sigma=\chi(A/A_{buckling}-1)$.

  The shell is elastic only in a narrow area range. The lower limit is $A_{buckling}$ for the area, or equivalently $R_{buckling}$ for the radius. The upper limit radius is fixed by the maximum surface tension, which is $\sigma_{break-up}$ before rupture of the shell giving $R_{break-up}=R_{buckling}(1+\sigma_{break-up}/\chi)^{1/2}$, or σ_{water} after rupture giving $R_{ruptured}=R_{buckling}(1+\sigma_{water}/\chi)^{1/2}$. The elastic regime holds only in a narrow range of radii, since χ is usually large compared to $\sigma_{break-up}$ or σ_{water}. The value of the elastic modulus can also incorporate the presence of any solid-like shell material that sustains tensile stress (such as the polyethyleneglycol polymer in SonoVue® contrast agent bubbles[5]). We assign a constant elastic modulus in this state, slightly caricaturing the quasi-static profiles of Fig. 1, a simplification of the model to facilitate calculation.

  Within this regime the surface tension is a linear function of the area, or of the square of the radius, and for small variations around a given radius R_0, it can be written as:

$$\sigma(R)=\sigma(R_0)+\chi\left(\frac{R^2}{R_0^2}-1\right)\simeq\sigma(R_0)+2\chi\left(\frac{R}{R_0}-1\right)\quad\text{when } |R-R_0|\ll R_0. \tag{1}$$

  The lipid monolayer behaves as if composed of a thin solid

and elastic material, see the appendix for the derivation of the tension of a thin elastic shell.

- Ruptured state, $\sigma=\sigma_{\text{water}}$.
  A fast expansion, such as the one triggered on a bubble by an ultrasonic pressure pulse, does not allow much time for any phase change and the monolayer is likely to break at a critical tension $\sigma_{\text{break-up}}$, exposing bare gas interfaces to the liquid. The bare interface has a tension value of σ_{water}. The break-up tension can be higher than σ_{water}, since any polymer component confers more cohesion to the shell, and shifts the break-up to higher tensions. The introduction of a high tension break-up was motivated by the observation of resistant bubbles, as will be exposed further.
  After break-up we assume that surface tension relaxes to σ_{water}. Even if the phospholipid monolayer rafts are likely to display non-isotropic tensions and shear stresses (being solid), the expansion is uniform before rupture, and the stress is likely to remain close to uniformity on average. The average tension value is settled in this case by the local mechanical equilibrium between the solid rafts and the bare interfaces, the latter pulling with the tension σ_{water}.

B. Dynamics of the coated bubble

During the oscillation, the dynamical surface tension will vary, since it is a function of the bubble area and therefore of the bubble radius. We therefore write the effective surface tension $\sigma(R)$ to emphasize this dependence. In motion, the balance of normal stresses at the interface reads

$$P_g(t) - P_l(t) = \frac{2\sigma(R)}{R} + 4\mu\frac{\dot{R}}{R} + 4\kappa_s\frac{\dot{R}}{R^2}, \tag{2}$$

with P_g as the gas pressure in the bubble, P_l as the liquid pressure, μ as the surrounding liquid viscosity, and κ_s as the surface dilatational viscosity from the monolayer. The first term on right-hand side is the capillary pressure term, while the second is the stress arising from the frictions in the liquid and the third from frictions in the shell. The last term was initially derived for a layer of finite and constant thickness ϵ ($\epsilon \ll R$) by Morgan *et al.*,[15] the dilatational viscosity writing $\kappa_s=3\epsilon\mu_{\text{lipid}}$, with μ_{lipid} as the bulk lipid viscosity. Here we use only κ_s to describe the monolayer shell surface viscosity, following Chatterjee and Sarkar.[16] In this model κ_s does not depend on the surface area, nor does it exhibit any hysteresis. Note that the shear viscosity of the surface does not come into play in the present situation, because of the radial motion of the bubble.

The Laplace capillary pressure term writes $2\sigma(R)/R$ including the effective surface tension, *without any additional terms*, contrary to a previous statement in an article by Glazman,[17] who expressed the capillary pressure by the erroneous expression $2\sigma/R+\partial\sigma/\partial R=2/R[\sigma+\chi(R_0/R)^2]$. We demonstrate here why: the capillary overpressure derives from the mechanical equilibrium of all forces acting on the interface (of vanishing mass), that is the infinitesimal work δW of the forces cancels out for small bubble radius variation. By definition, the work associated with a variation dA of the area is σdA,[18] while the pressure work from a variation dV of the volume is $-(P_g-P_l)dV$. Owing to the mechanical equilibrium of the interface, the sum of these works vanishes, and we obtain the static capillary term of Eq. (2). In the analysis by Glazman, the surface work is expressed incorrectly by $\sigma dA+Ad\sigma$ (instead of σdA) from the differentiation of a surface potential energy $E=\sigma A$: actually this last expression of the surface potential energy ($E=\int \delta W_{surface}$ by definition) is valid only when σ is constant.

The popular model of Morgan *et al.*[15] for coated microbubbles improves the description of viscous frictions, but is based on the analysis of Glazman for the elasticity of the lipid shell, equivalent to the introduction of an effective surface tension $\sigma(R)=\sigma_0+\chi(R_0/R)^2$ that fails to describe a coated bubble. Physically it would mean that surface tension always decreases when the bubble is inflated, in contrast with the behavior of lipid monolayers or elastic solid shells.

The hydrodynamics of the liquid motion around the bubble is modeled by the (modified) Rayleigh-Plesset equation $\rho_l\left(R\ddot{R}+\frac{3}{2}\dot{R}^2\right)=P_l(t)-P_0-P_{\text{ac}}(t)-(R/c)[dP_g(t)/dt]$, with P_0 as the ambient pressure, $P_{\text{ac}}(t)$ as the acoustic pressure, and c as the velocity of sound in the liquid. This equation proved to be accurate and robust even in the extreme conditions of sonoluminescence.[19] We choose an ideal polytropic ideal gas law $P_g \propto R^{-3\kappa}$, with κ as the polytropic gas exponent. It is 1 for bubbles behaving isothermally, and equal to the ratio of specific heats for bubbles behaving adiabatically[20] (close to 1.095 for SF_6). In the following, the thermal diffusion length in the gas during a period being small compared to the radius, we use the adiabatic version.

Combining the Rayleigh-Plesset equation and the polytropic gas law with the boundary condition (2) we obtain the model for the bubble dynamics

$$\rho_l\left(R\ddot{R}+\frac{3}{2}\dot{R}^2\right) = \left[P_0+\frac{2\sigma(R_0)}{R_0}\right]\left(\frac{R}{R_0}\right)^{-3\kappa}\left(1-\frac{3\kappa}{c}\dot{R}\right) - P_0 - \frac{2\sigma(R)}{R} - \frac{4\mu\dot{R}}{R} - \frac{4\kappa_s\dot{R}}{R^2} - P_{\text{ac}}(t), \tag{3}$$

with R_0 the equilibrium radius of the bubble. This equation is identical to a free gas bubble equation, except from the effective surface tension $\sigma(R)$ term and the shell viscosity term. The tension expressed in our monolayer model described above, and expressed here in terms of the bubble radius writes:

$$\sigma(R) = \begin{cases} 0 & \text{if } R \leqslant R_{\text{buckling}} \\ \chi\left(\dfrac{R^2}{R_{\text{buckling}}^2}-1\right) & \text{if } R_{\text{buckling}} \leqslant R \leqslant R_{\text{break-up}} \\ \sigma_{\text{water}} & \text{if ruptured and } R \geqslant R_{\text{ruptured}}. \end{cases} \tag{4}$$

The third regime appears after rupture of the shell, when $\sigma_{\text{break-up}}$ has been reached (see broken line in Fig. 2).

For small vibration amplitudes within the tensed elastic state, the surface tension can be linearized around a constant value, with $\sigma(R) \simeq \sigma(R_0)+2\chi(R/R_0-1)$, from Eq. (1). Implemented in the dynamical equation its yields the same

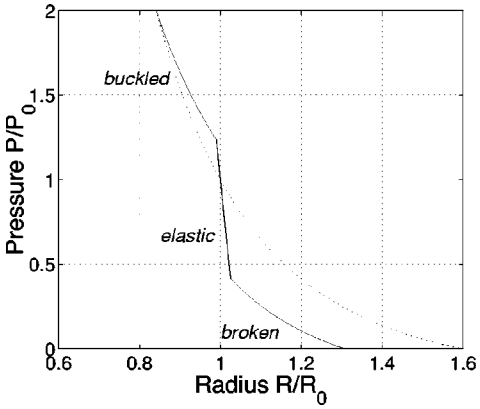

FIG. 3. Ambient pressure vs equilibrium radius for a coated bubble (continuous line) and a free gas bubble (dotted line). At atmospheric pressure, the bubble radius is $R_0=2$ μm. The coated bubble is initially in the elastic state ($R_{\text{buckling}}=1.98$ μm, $\chi=1$ N/m).

pressure term $-2\sigma(R)/R=-2\sigma(R_0)/R-4\chi(1/R_0-1/R)$ as in the model proposed by de Jong *et al.*[21] for thin elastic shells. The shell stiffness coefficient S_p they introduced is simply related to the present shell elasticity by $S_p=2\chi$, while their shell friction coefficient writes $S_f=12\pi\kappa_s$. We stress here again that the model by de Jong *et al.*[21] is limited to small amplitudes of vibration (for effective tensions bounded between 0 and σ_{water}, or for R in between R_{buckling} and R_{collapse}), while the present model extends the oscillation to unbounded, large amplitudes.

C. Implications of the model: Bubble compressibility

The effective tension model drastically changes the compressibility of the bubble. For slow variations of the ambient pressure P, at frequencies small compared to the resonance frequency, we can compute the equilibrium radius response, see Fig. 3, setting $\dot{R}=0$ in Eqs. (3) and (4).

From the equilibrium, we also derive the compression modulus of the bubble, K_V, with

$$K_V=-V\left(\frac{dP}{dV}\right)=\begin{cases}\kappa P & \text{for the buckled state}\\ \kappa P+\dfrac{4}{3}\dfrac{\chi}{R} & \text{for the elastic state}\\ \kappa P+\dfrac{3\kappa-1}{3}\dfrac{2\sigma_{\text{water}}}{R} & \text{for the free bubble/broken shell state}\end{cases} \tag{5}$$

with V as the bubble volume, a polytropic exponent κ close to 1 for slow and isothermal compressions, and in the limit of $\chi \gg \sigma_{\text{water}}$ (usual for phospholipids). The compression modulus is much higher when the bubble is in the elastic state: this is reflected in the much steeper slope of the curve in Fig. 3. When the pressure is increased enough the bubble buckles, and becomes very compressible, even more than an uncoated free gas bubble of the same radius (whose internal pressure is increased by capillarity).

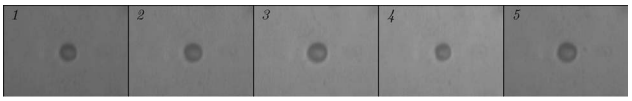

FIG. 4. Consecutive images of a contrast agent bubble from the high speed camera Brandaris operated at 14.3 million frames per second (time intervals between images are thus 69.8 ns), during one ultrasound cycle, of frequency 2.6 MHz. The bubble radius is initially 1.95 μm, and frame number 4 shows the bubble compression.

The change in compressibility is reflected on the dynamics of small amplitude oscillations as well. The linearization of the equations, setting $R(t)=R_0[1+x(t)]$, provides a damped oscillator equation $\ddot{x}+2\gamma\dot{x}+\omega_0^2 x=-P_{\text{ac}}(t)/\rho_l R_0^2$, with a damping coefficient $\gamma=2\mu/\rho_l R_0^2+2\kappa_s/\rho_l R_0^3+3\kappa[P_0+2\sigma(R_0)/R_0]/2c\rho_l R_0$, and an eigenfrequency simply writing

$$\omega_0^2=\frac{3}{\rho_l R_0^2}K_V. \tag{6}$$

In the free bubble state, this equation provides the Minnaert frequency as expected. It can be concluded that bubbles in the elastic state have a much higher resonance frequency than free or buckled bubbles, because their compression modulus is higher, consistently with the derivation of de Jong.[21]

III. RESULTS

A. Compression-only behavior

At small acoustic amplitudes, the model presented earlier provides a linear radius response to the pressure similar to other Rayleigh-Plesset models with constant surface tension.

Under large pressure amplitudes, the bubble will experience an original non-linear response. It will likely buckle in its compression phase, which cancels out any surface tension. On the other hand, the surface tension rapidly rises during the expansion phase, and this asymmetry in surface tension provides an asymmetry in capillary pressure, especially strong for small bubbles. The radius response curve displays this asymmetry by a "compression-only" behavior.

Recent experiments, realized with the high-speed camera Brandaris 128,[22] reveal the existence of such asymmetric oscillations of bubbles. The experiment was conducted as follows: SonoVue® and BR14 contrast bubbles, supplied by Bracco Research SA, Geneva, Switzerland, were prepared in the vial about 24 h prior to the recording of their dynamics. Both types of bubbles present a phospholipidic coating, SonoVue® containing SF_6 gas,[5] while BR14 contains the even less soluble C_4F_{10} gas.[23] The contrast bubbles were led through a capillary fiber inside a small water-filled container. An Olympus microscope with a 60× high resolution water immersed objective and a 2× magnifier produced an image of the contrast bubbles. The image was then relayed to the high speed framing camera Brandaris 128. A broadband single element transducer was mounted at 75 mm from the capillary. A Tektronix AWG 520 arbitrary waveform generator provided a signal amplified by an ENI A-500 amplifier. The bubble response was investigated with sequential ultrasound bursts of 8 cycles at frequencies ranging from

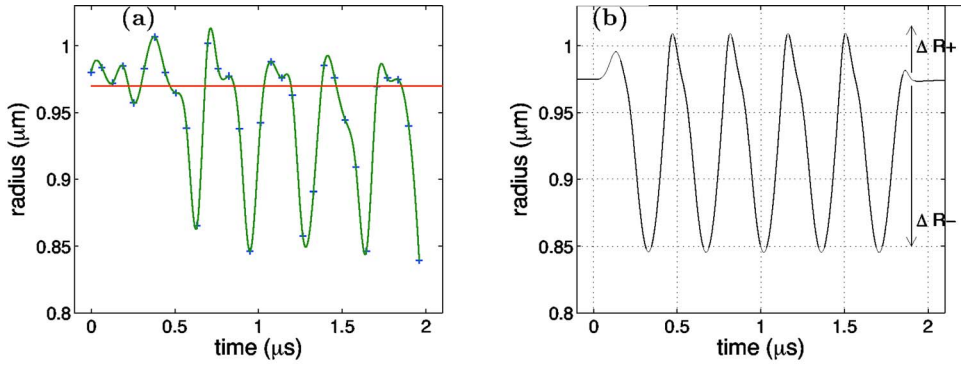

FIG. 5. (Color online) (a) Experimental recording of the radius of a SonoVue® bubble vs time, with the fast framing camera Brandaris (beginning of a 2.9 MHz pulse with an acoustic pressure of 130 kPa). (b) Simulation. The fitted shell parameters are $R_{buckling}=R_0=0.975$ μm, $\chi=1$ N/m, $\kappa_s=15\times10^{-9}$ N and $\sigma_{break\text{-}up}>1$ N/m (resistant shell). The liquid properties are $\rho_l=10^3$ kg/m^3, $\mu=0.001$ Pa s, $c=1480$ m/s, and the polytropic gas exponent is $\kappa=1.095$.

1.5 to 5 MHz. The camera was operated at a framing rate of 15 million frames per second, resolving the insonified microbubble dynamics. From the images (see Fig. 4) the radius versus time curves for each individual bubble were extracted [Fig. 5(a)], from which the compression-only behavior is apparent.

This phenomenon is very well modeled with our effective surface tension model, see Fig. 5(b), assuming the bubble to be initially in a tension-less state ($R_{buckling}=R_0$), and allowing the shell to support elevated tensions. Note that the fitted elastic modulus and shell viscosity of this shell are of the same order of magnitude than the average ones from attenuation measurements on bubble populations by Gorce *et al.*,[24] who deduced an average shell elasticity $\chi=S_p/2=0.55$ N/m and shell friction $\kappa_s=S_f/12\pi=7.2\times10^{-9}$ N.

B. Aging of micro-bubbles: Effect on the oscillation response

The initial effective tension of the monolayer depends on the history of the bubble. During their formation in the vial, lipid molecules are adsorbed at the interface, which reduces the effective surface tension, in proportion to the surface concentration n/A of adsorbed lipid molecules. The bubble is initiated in the tensed elastic state, its area being above the buckling area, $A_{buckling}=n*a_{buckling}$.

Dissolution of the gas in the surrounding liquid will "deflate" the bubble and reduce its area towards a tension-less state (like the deflation of a rubber balloon), below which the bubble will buckle. In the tension-less state dissolution is much slower, since the capillary overpressure (typically an atmospheric pressure for micrometric bubbles) vanishes and the rate of radius decrease is proportional to inside pressure (which determines the dissolution concentration in the liquid according to Henry's law). Bubbles therefore *spontaneously tend to their buckling radius*, and then shrink much more slowly, compared to bubbles of constant surface tension. The reduction of surface tension is the main mechanism to account for increased longevity from the coating, since the gas permeability of 16- and 18-carbons phospholipids coatings is high.[8]

Experiments show that asymmetric oscillations become more pronounced in the course of dissolution, see Fig. 6. Our interpretation is that the bubble reaches the tension-less state, where buckling occurs. According to the present model, the asymmetry is the signature of the variation in surface tension during each cycle, and this variation is the highest near buckling.

The asymmetry can be monitored by the ratio $\Delta R^+/\Delta R^-$ of the positive and negative radius excursions [defined by $\Delta R^+=\max(R)-R_0$ and $\Delta R^-=R_0-\min(R)$, both materialized in Fig. 5(b)]. Simulations demonstrate indeed that the compression-only asymmetry ($\Delta R^+/\Delta R^-<1$), is the more pronounced when $R_0/R_{buckling}\sim1$ (see Fig. 7), the tension asymmetry during the oscillation being maximal.

This behavior is to be contrasted with the large amplitude oscillation of bubbles with a constant surface tension, which tends to produce higher positive excursions. It is seen in the same figure when the bubble radius is well above $R_{buckling}$ (free bubble state, $\sigma=\sigma_{water}$) or well below $R_{buckling}$ (tension-less state, $\sigma=0$). The response curve slightly depends on frequency: varying the frequency between 1 and 4 MHz changes $\Delta R^+/\Delta R^-$ by about 10%.

Repeated pulses on a bubble accelerate the gas dissolution, as evidenced in Fig. 6 by the sudden decrease after the first pulse and the subsequent pulses. Two mechanisms could account for this effect. First, the initial pulses may expel

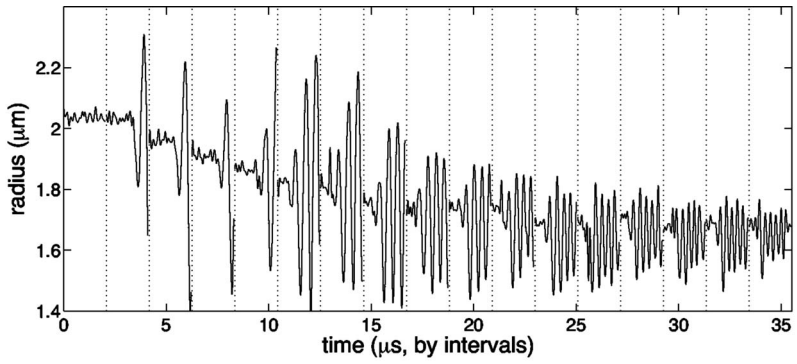

FIG. 6. Experimental recordings of repeated acoustic pulses of 100 kPa on a single bubble, separated by 50 ms (break of time at vertical lines). The oscillation asymmetry increases pulse after pulse. (Frequency is increasing from 1.5 to 4 MHz, inducing amplitude changes).

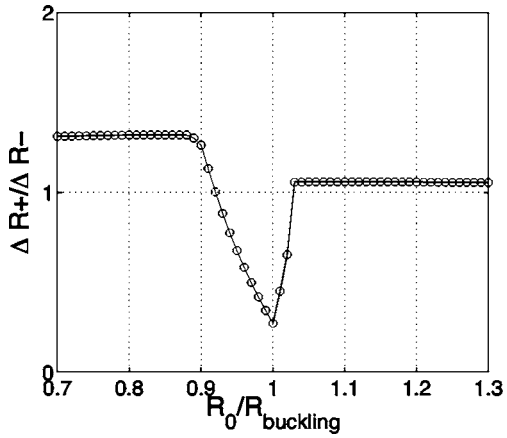

FIG. 7. Simulated asymmetry of the oscillation for varying starting radii. Acoustic pulse and shell properties: same as Fig. 5.

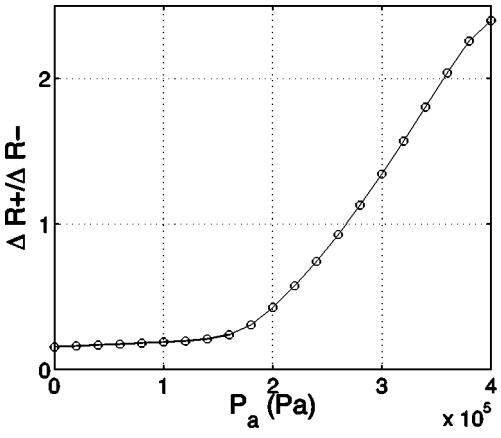

FIG. 9. Effect of an increasing acoustic pressure on the asymmetry of the response [same parameters as in Fig. 8(b)].

some lipid molecules and reduce the buckling radius, to which the bubble will relax. Another explanation would be an "inverse" rectified-diffusion generated by compression-only behaviors. The gas pressure increases during the compression phase, while it remains close to the pressure at rest during expansion (a symmetric oscillation would alternately compress and expand the gas). The concentration of gas in the liquid near the interface being proportional to gas pressure (Henry's law), the asymmetry, even small, tends to force more gas out of the bubble. This "inverted" rectified-diffusion would be the opposite of the usual rectified-diffusion effect that counteracts dissolution for free gas bubbles.[25]

A quantitative evaluation of this effect follows from the expression of the rate of dissolution of an oscillating bubble[25,26]

$$\frac{d}{dt}\overline{R(t)} = \frac{Dc_0}{\rho_g \overline{R(t)}^2}\left[\frac{c_\infty}{c_0} - \frac{\overline{P_g(t)R(t)^4}}{P_0\overline{R(t)^4}}\right] \times \left\{\int_0^\infty \frac{dh'}{\overline{[3h'+R(t)^3]^{4/3}}}\right\}^{-1}, \quad (7)$$

where the overline is the average over one period, this equation being valid for an evolution slow at the scale of the period. The diffusivity of the gas is D, its volumic mass ρ_g, its saturation concentration c_0, and its concentration far from the bubble c_∞. The last factor containing an integration along the variable h' does not change sign, and tends to R^4 for small amplitude oscillations. A compression-only signal produces a stronger "averaged" pressure term $\overline{P_g(t)R(t)^4}/\overline{R(t)^4}$ [for instance it amounts to $1.2P_0$ from the simulation in Fig. 5(b)], which accelerates dissolution. Even at R_{buckling}, where the capillary overpressure vanishes, inverted rectified diffusion can force dissolution in a fully saturated liquid with $c_\infty/c_0=1$.

C. Rupture of the shell

The shell can withstand finite tensions only in its shell: starting from a compression-only signal and increasing the acoustic pressure step by step shows that a strong positive radius excursion suddenly appears above a critical pressure [see Fig. 8(a)]. In this new state, the bubble oscillates as a free bubble: we interpret this behavior as the effect of the shell rupture.

To model the rupture, we assume that above a critical tension, $\sigma_{\text{break-up}}$, the shell breaks up and that part of the bubble surface is uncovered. Once this threshold has been reached, the surface tension upper bound will be the surface tension of water, σ_{water}. We can therefore simulate the effect of an increasing acoustic pressure on a bubble [see Fig. 8(b)].

The compression-only behavior ($\Delta R^+/\Delta R^- < 1$) is interrupted by the break-up of the shell: the non-linear behavior then favors positive excursions of the radius, as seen in experiment, as for standard large pressure Rayleigh-Plesset dynamics (see Fig. 9).

IV. CONCLUSIONS

We presented a simple model for the dynamical properties of coated contrast agents bubbles, with three parameters:

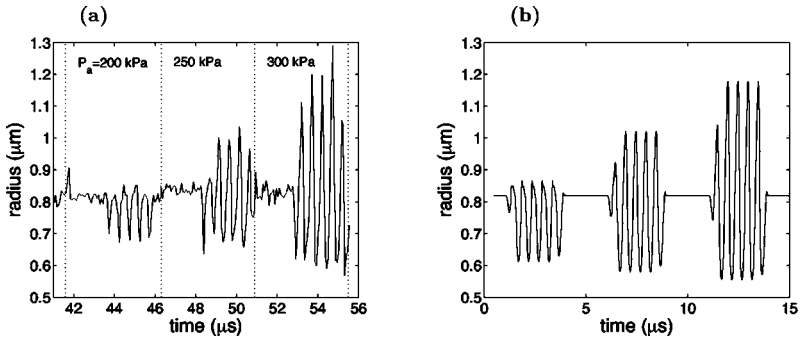

FIG. 8. (a) Experimental recordings of a BR14 bubble response to repeated 2 MHz pulses separated by 60 ms, with an increasing acoustic pressure. (b) Simulation with the same acoustic pressures. The fitted shell parameters are $R_{\text{buckling}}=R_0=0.82\ \mu$m, $\chi=1$ N/m, $\kappa_s=7.2\times10^{-9}$ N, while the critical break-up is $\sigma_{\text{break-up}}=0.13$ N/m.

a buckling surface radius, a shell compressibility, and a break-up shell tension. It predicts a compression-only behavior of the bubble, a highly non-linear response. It occurs when its radius is close to the buckling radius, a state that naturally occurs with dissolution of gas, or that can be accelerated by repeated pulses. High-frequency image recordings with lipid coated microbubbles reveal the existence of such asymmetric oscillations, and validate the model. The break-up of the shell is modeled by a third parameter, a finite tension of the bubble shell above which bare interfaces are created, with a corresponding change in bubble dynamics.

Possible applications of the model include: the characterization of coated microbubbles, the description of acoustic echoes and their use in non-linear or pulse-inversion imaging, and the prediction of the effect of repeated pulses or of long-term experiments.

ACKNOWLEDGMENTS

The authors would like to thank Joris Timmermans for his help in computations. They appreciated fruitful discussions with François Graner and Wouter den Otter.

APPENDIX: COMPARISON WITH THE ELASTICITY OF A SOLID SHELL LAYER

Like monolayer coatings, the elasticity of a thin solid shell of thickness $\epsilon \ll R$ is characterized by a two-dimensional compression modulus $\chi = A(d\sigma/dA)$, where σ is the isotropic in-plane tension (shear of the surface does not occur with a radial expansion, and bending is neglected assuming an initial curvature close to the spontaneous curvature). Additionally, the solid shell has two interfaces, with a surface tension σ_1 for the inner interface and σ_2 for the outer interface. The mechanical equilibrium balance for any small change in bubble area around the tensionless shell area A_0 reads $\delta W = \chi(A/A_0 - 1)dA + \sigma_1 dA + \sigma_2 dA - (P_g - P_l)dV = 0$, from which we obtain the pressure jump at the liquid-gas interface $P_g - P_l = 2[\sigma_1 + \sigma_2 + \chi(A/A_0 - 1)]/R$. The effective surface tension of the shell thus reads

$$\sigma = \sigma_1 + \sigma_2 + \chi\left(\frac{R^2}{R_0^2} - 1\right), \tag{A1}$$

it is a linear function of the bubble area, like in the lipid *monolayer* coated bubble model [Eq. (1) for the elastic state, with $\sigma(R_0) = \sigma_1 + \sigma_2$].

The model for a thick elastic shell by Church[27] provides the same effective surface tension law when the shell thickness ϵ tends to be small compared to the radius. In this model the shell has a bulk shear modulus G_s and is incompressible in volume (the thickness thus varies around its equilibrium value during the oscillation). From the Church model at small thicknesses we find that the shell contribution can be expressed with an effective tension law as in Eq. (A1), using a two-dimensional elastic modulus $\chi = 3G_s\epsilon$, which is a classical result of the elasticity of thin plates.[28]

[1] J. M. Crane and S. B. Hall, "Rapid compression transforms interfacial monolayers of pulmonary surfactant," Biophys. J. **80**, 1863 (2001).
[2] A. L. Klibanov, "Ultrasound contrast agents: Development of the field and current status," Top. Curr. Chem. **222**, 73 (2002).
[3] S. Lee, D. H. Kim, and D. Needham, "Equilibrium and dynamic interfacial tension measurements at microscopic interfaces using a micropipet technique. 2: Dynamics of phospholipid monolayer formation and equilibrium tensions at the water-air interface," Langmuir **17**, 5544 (2001).
[4] J. M. Crane, G. Putz, and S. B. Hall, "Persistence of phase coexistence in disaturated phosphatidylcholine monolayers at high surface pressures," Biophys. J. **77**, 3134 (1999).
[5] M. Schneider, M. Arditi, M.-B. Barrau, J. Brochot, A. Broillet, R. Ventrone, and F. Yan, "BR1: A new ultrasonic contrast agent based on sulfur hexafluoride-filled microbubbles," Invest. Radiol. **30**, 451 (1995).
[6] F. Pétriat, E. Roux, J.-C. Leroux, and S. Giasson, "Study of molecular interactions between a phospholipidic layer and a *p*H-sensitive polymer using the langmuir balance technique," Langmuir **20**, 1393 (2004).
[7] M. I. Sández, A. Suárez, and A. Gil, "Surface pressure-area isotherms and fluorescent behavior of phospholipids containing labeled pyrene," J. Colloid Interface Sci. **250**, 128 (2002).
[8] M. A. Borden and M. L. Longo, "Dissolution behavior of lipid monolayer-coated, air-filled microbubbles: Effect of lipid hydrophobic chain length," Langmuir **18**, 9225 (2002).
[9] A. Saint-Jalmes, F. Graner, F. Gallet, and B. Houchmandzadeh, "Buckling of a bidimensional solid," Europhys. Lett. **28**, 565 (1994).
[10] A. Saint-Jalmes and F. Gallet, "Buckling in a solid langmuir monolayer: Light scattering measurements and elastic model," Eur. Phys. J. B **2**, 489 (1998).
[11] D. H. Kim, M. J. Costello, P. B. Duncan, and D. Needham, "Mechanical properties and microstructure of polycrystalline phospholipid monolayer shells: Novel solid microparticles," Langmuir **19**, 8455 (2003).
[12] P. B. Duncan and D. Needham, "Test of the epstein-plesset model for gas microparticle dissolution in aqueous media: Effect of surface tension and gas undersaturation in solution," Langmuir **20**, 2567 (2004).
[13] F. Graner, S. Perez-Oyarzun, A. Saint-Jalmes, C. Flament, and F. Gallet, "Phospholipidic monolayers on formamide," J. Phys. II **5**, 313 (1995).
[14] G. Gaines and L. George, *Insoluble Monolayers at Liquid-Gas Interfaces* (Interscience, New York, 1966).
[15] K. E. Morgan, J. S. Allen, P. A. Dayton, J. E. Chomas, A. L. Klibanov, and K. W. Ferrara, "Experimental and theoretical evaluation of microbubble behaviour: Effect of transmitted phase and bubble size," IEEE Trans. Ultrason. Ferroelectr. Freq. Control **47**, 1494 (2000).
[16] D. Chatterjee and K. Sarkar, "A newtonian rheological model for the interface of microbubble contrast agents," Ultrasound Med. Biol. **29**, 1749 (2003).
[17] R. E. Glazman, "Effects of an adsorbed film on gas bubble radial oscillations," J. Acoust. Soc. Am. **74**, 980 (1983).
[18] P.-G. de Gennes, F. Brochard-Wyart, and D. Quéré, *Capillarity and Wetting Phenomena: Drops, Bubbles, Pearls, Waves* (Springer, New York, 2004).
[19] M. P. Brenner, S. Hilgenfeldt, and D. Lohse, "Single-bubble sonoluminescence," Rev. Mod. Phys. **74**, 425 (2002).
[20] A. Properetti, "Bubble phenomena in sound fields: Part one," Ultrasonics **22**, 69 (1984).
[21] N. de Jong, R. Cornet, and C. Lancée, "Higher harmonics of vibration gas-filled microspheres. part one: simulations," Ultrasonics **32**, 447 (1994).
[22] C. T. Chin, C. Lancée, J. Borsboom, F. Mastik, M. Frijlink, N. de Jong, M. Versluis, and D. Lohse, "Brandaris 128: A digital 25 million frames per second camera with 128 highly sensitive frames," Rev. Sci. Instrum. **74**, 5026 (2003).
[23] M. Schneider, A. Broillet, P. Bussat, N. Giessinger, J. Puginier, R. Ventrone, and F. Yan, "Grayscale liver enhancement in VX2 tumor-bearing rabbits using BR14, a new ultrasonographic contrast agent," Invest. Radiol. **32**, 410 (1997).
[24] J. M. Gorce, M. Arditi, and M. Schneider, "Influence of bubble size distribution on the echogenicity of ultrasound contrast agents: A study of Sonovue," Invest. Radiol. **35**, 661 (2000).
[25] S. Hilgenfeldt, D. Lohse, and M. P. Brenner, "Phase diagrams for sonoluminescing bubbles," Phys. Fluids **8**, 2808 (1996).
[26] M. Fyrillas and A. J. Szeri, "Dissolution or growth of soluble spherical oscillating bubbles," J. Fluid Mech. **277**, 381 (1994).
[27] C. C. Church, "The effects of an elastic solid surface layer on the radial pulsations of gas bubbles," J. Acoust. Soc. Am. **97**, 1510 (1995).
[28] D. Boal, *Mechanics of the cell* (Cambridge University Press, Cambridge, 2002).